Nanoscale Research Letters

NANO EXPRESS

Open Access

Bone Marrow Mesenchymal Stem Cell-Derived Exosomal MicroRNA-133a Restrains Myocardial Fibrosis and Epithelial–Mesenchymal Transition in Viral Myocarditis Rats Through Suppressing MAML1

Qiming Li[1*], Yunpeng Jin[1], Xiaoqi Ye[2], Wei Wang[1], Gang Deng[3] and Xiaojian Zhang[1]

Abstract

Myocarditis is a disease characterized by localized or diffuse inflammation of the myocardium without efficient treatment. This study explored the regulatory mechanism of microRNA-133 (miR-133) secreted from bone marrow mesenchymal stem cell-derived exosome (BMSC-Exo) on myocardial fibrosis and epithelial–mesenchymal transition (EMT) in viral myocarditis (VMC) rats through regulating mastermind-like 1 (MAML1). BMSCs in rats were isolated and cultured to identify their immune phenotype and osteogenic and adipogenic ability, and BMSC-Exo were extracted and identified. Exosomes were obtained through ultracentrifugation, which were identified by transmission electron microscope and western blot analysis. The rats were injected with Coxsackie B3 virus for preparation of VMC model, and cardiomyocytes were isolated, cultured and grouped in the same way as animal experiments (NC^{Exo}, Ad-miR-$133a^{Exo}$, Adas-miR-$133a^{Exo}$). In vivo and in vitro experiments were conducted to figure out the roles of exosomal miR-133a and MAML1 in inflammation, apoptosis, EMT, fibrosis, and cell viability. The targeting relationship between miR-133a and MAML1 was verified by dual luciferase reporter gene assay. BMSC-Exo raised miR-133a expression in VMC rats and effectively improved the VMC rat cardiac function and myocardial fibrosis, increased cardiomyocyte viability and inhibited the EMT process. Elevated miR-133a in exosomes strengthened the improvements. Silenced miR-133a effectively reversed the effects of BMSC-Exo on VMC rats. miR-133a targeted MAML1. Inhibition of MAML1 improved cardiac function and myocardial fibrosis in VMC rats and could reverse the effect of miR-133a-silenced exosomes on VMC rats. Our study suggests that elevated exosomal miR-133a suppresses myocardial fibrosis and EMT in rats with VMC via down-regulating MAML1, thereby inhibiting the progression of myocarditis.

Keywords: Viral myocarditis, MicroRNA-133a, Bone marrow mesenchymal stem cells, Exosomes, MAML1, Fibrosis, Epithelial–mesenchymal transition

Introduction

Myocarditis is considered as an inflammatory illness of the heart muscle cells [1]. Myocarditis is obviously more familiar in male in contrast with female [2]. Viral myocarditis (VMC) is a main factor leading to dilated cardiomyopathy (DCM) and sudden death in young people [3]. The clinical performance of myocarditis is various, ranging from asymptomatic states with ambiguous signs

*Correspondence: 8015006@zju.edu.cn
[1] The Department of Cardiology, The Fourth Affiliated Hospital of Zhejiang University School of Medicine, N1 Shangcheng Road, Yiwu 322000, Zhejiang, China
Full list of author information is available at the end of the article

and symptoms to serious myocardial destruction by virus and immune cells suffering from cardiogenic shock and arrhythmias [1]. Myocarditis can be induced by a variety of infectious elements, consisting of viruses, bacteria, Chlamydia, rickettsia, fungi, and protozoa, together with noninfectious inducers. Among which, viral infection has been the most common cause, especially in children [4]. Coxsackie B3 virus (CVB3), as the most crucial virus that leads to myocarditis, can result in oxidative stress response and apoptosis in the pathogenesis of VMC, but special treatment of VMC has not been reported yet [5]. Moreover, the pathogenesis of VMC is not well documented, and an exact clinical treatment is also lacking [3]. Therefore, novel targets are urgently needed to improve prognosis of the disease.

MicroRNAs (miRNAs) are endogenous noncoding RNAs that can regulate the expression of protein-coding genes [6]. MiR-133a, as one of cardiac-specific miRNAs, is implicated in the heart development and some cardiovascular diseases, containing myocardial infarction (MI) [7]. In addition, miR-133a is the one that is aberrantly expressed in chronic Chagas disease cardiomyopathy [8]. Moreover, miR-133a level in myocardium is connected with inflammation, left ventricular function, and clinical outcome in inflammatory cardiomyopathy [9]. MiRNAs were found in exosomes derived from mouse and human mast cells [10]. Exosomes, nanosized vesicles released by most cell kinds are found in different biological fluids [11]. Exosomes can transfer their cargo to recipient cells, which has been shown to change the biochemical composition and signaling pathways of the recipient cells [12, 13]. Evidence has shown that changed exosomal miRNAs are connected with the pathogenesis of CVB3-induced myocarditis [14]. It has been addressed that exosomal miR-125b-5p from hypoxia-conditioned bone marrow mesenchymal stem cells reduces cardiomyocyte apoptosis and enhances ischemic cardiac repair [15]. Moreover, exosomal miR-25-3p from MSCs alleviates MI through reducing cardiomyocyte apoptosis and inflammatory response [16]. Of interest, exosomal cardiac-expressed miR-133a is connected to the cardiac troponincardiac troponin-I [17]. Mastermind-like 1 (MAML1) was a cross-screened downstream gene of miR-133a in our study which has been reported to involve in myocardial ischemia/reperfusion (I/R) injury [18]. Also, a recent study has mentioned that MAML1 knockdown possesses the anti-fibrotic function in liver fibrosis [19].

Illuminated by previous studies, it is wondered that whether BMSCs-derived exosomal miR-133a could mediate myocarditis. Therefore, this study was started with a hypothesis that miR-133 shuttled by BMSC-derived exosome (BMSC-Exo) ameliorates myocardial fibrosis and epithelial–mesenchymal transition (EMT) in VMC rats through regulation of MAML1.

Materials and Methods

Ethical Approval

The study was allowed by the Institutional Animal Care and Use Committee of The Fourth Affiliated Hospital of Zhejiang University School of Medicine. Animals were treated humanely.

Isolation of BMSCs

Experimental animals were mature specific pathogen-free (SPF) grade Sprague–Dawley (SD) male rats (Experimental Animal Center of Zhejiang University School of Medicine, Zhejiang, China). The rats were euthanized by intraperitoneal injection with pentobarbital sodium and sterilized with 75% alcohol. The femur and tibia were taken out on an ultra-clean table, the muscle and connective tissues were removed, and the marrow cavity was rinsed repeatedly with low glucose Dulbecco's Modified Eagle Medium (DMEM). The liquid was centrifuged to collect the precipitates which were re-suspended and incubated for 24 h (the medium was changed every 2–3 d). When growing to the logarithmic phase, BMSCs were detached with 0.25% trypsin (Gibco, Carlsbad, California, USA), centrifuged and resuspended in MSC culture solution (Cyagen Biosciences Inc., Guangzhou, China). The suspension was passaged at a ratio of 1:2. The above operation was repeated, and the 4th passage BMSCs were used for subsequent experiments.

Identification of BMSCs

The surface antigens of the 4th passage BMSCs in logarithmic growth were identified by flow cytometry. The BMSCs were detached with 0.25% trypsin (1 mL) containing ethylene diamine tetraacetic acid, centrifuged, re-suspended with appropriate phosphate-buffered saline (PBS) and centrifuged at 151 g. The BMSCs were then re-suspended with PBS containing 2% fresh fetal bovine serum (FBS) (Gibco) to make a single-cell suspension. FITC-CD34, PE-CD29, and PE-CD44 monoclonal antibody (5 μL each, BD Biosciences, Franklin Lakes, NJ, USA) were incubated with the cell suspension (100 μL), centrifuged at 151 g, re-suspended with 500 μL PBS containing 1% paraformaldehyde and fixed for 30 min. The background markers were identified via using monoclonal antibodies from the homotype control.

Flow cytometry: the single-cell suspension was fixed and centrifuged at 151 g. Then the BMSCs were re-suspended with PBS containing 1% paraformaldehyde, tested on the MACS Quart flow cytometer and analyzed by the corresponding software.

Induction of Osteogenesis and Adipogenesis of BMSCs

BMSCs in the 4th passage were seeded into 6 well-plates with 200 cells/mL. The osteoblast induction solution and adipogenic induction solution (Cyagen Biosciences Inc.) were added into BMSCs of 60–70% confluence. BMSCs in other two wells were not added with induction liquids as controls. The BMSCs were induced for 14 days and fixed with 4% paraformaldehyde. Then the differentiated osteoblasts and adipocytes were implemented with Alizarin red staining and oil red O staining (Wuhan Pulande Biological Technology Co., Ltd., Wuhan, China), and observed under a microscope.

Exosome Isolation and Identification

BMSCs in the 4th passage were cultured for 48 h to harvest the supernatant which was then centrifuged (800 g and 2000 g), filtrated with 0.22 μm and 100,000 MW filter membranes, and centrifuged (100,000 g) to collect the precipitates. Then, the precipitates were re-suspended with PBS, centrifuged at 100,00 g again to obtain exosome precipitation. The BMSC-Exo suspension in PBS were subjected to concentration detection by bicinchoninic acid (BCA) and exosome maker protein detection (CD63, CD81 and CD9) by western blot analysis (Proteintech, Chicago, IL, USA).

Recombinant Adenovirus Infection Mediates miR-133a Gene Modification of BMSCs

BMSCs were passaged overnight. The normal control (equal amount of PBS), the miR-133a negative control (NC), the miR-133a over-expression (Ad-miR-133a), and miR-133a low-expression (Adas-miR-133a) (Hanbio Biotechnology Co., Ltd., Shanghai, China) were transfected with BMSCs in line with 100 multiplicity of infection (MOI). The BMSCs were cultured, and the corresponding exosomes (NC^{Exo}, NC^{Exo}, Ad-miR-133a^{Exo}, and Adas-miR-133a^{Exo}) were obtained through ultracentrifugation [20].

Establishment of VMC Model in Rats and Grouping of Experimental Animals

Mature male SPF-grade SD rats were divided into 10 groups, with eight rats each. Coxsackievirus B3 (CVB3) was provided by the Institute of Medical Biotechnology, Chinese Academy of Medical Sciences (Beijing, China).

CVB3 (10 mg/kg) was intraperitoneally injected into rats while PBS or BMSC-Exo (100 μg) was injected through the tail vein. Normal rats for controls were injected with CVB3 culture solution and PBS. Rats injected with 10 mg/kg CVB3 were further injected with PBS, MSC^{exo}, NC^{Exo}, Adas-miR-133a^{Exo}, Ad-miR-133a^{Exo}, si-NC, or si-MAML1 (RIBOBIO, Guangzhou, China).

The rats were continuously injected for 7 days and the eyeball blood was obtained. The blood was centrifuged and the serum was collected, sub-packaged, and stored at − 20 °C. After the rats were euthanized, the heart specimens were taken, fixed with 10% formaldehyde, dehydrated with gradient alcohol, cleared with xylene and embedded with paraffin, sectioned for histological observation. A part of sections were placed at − 80 °C as the molecular biology experiments materials.

Echocardiography

On the 7th day after virus injection, the rats were intraperitoneally injected with pentobarbital sodium 25 mg/kg. After complete anesthesia, the limb lead of the electrocardiogram machine connected with the electrode needle was inserted subcutaneously at the ends of the limbs of the rats, and the limb lead electrocardiogram was recorded. Then, the rats were fixed on the supine position slightly to the left, the chest was depilated, and the II lead electrocardiogram was connected to obtain the Doppler spectrum of the blood flow pulse of the aorta in the parasternal four-chamber heart section. Indicators included left ventricular posterior wall thickness (LVPW), left ventricular end-systolic diameter (LVIDs), left ventricular shortening fraction (FS), and left ventricular ejection fraction (LVEF).

Hematoxylin–Eosin (HE) Staining

The tissues were fixed with 4% paraformaldehyde, dehydrated, cleared, and embedded with paraffin. Then the 4-μm sections were de-waxed, stained with hematoxylin (Servicebio, Wuhan, China), differentiated with 1% hydrochloric acid alcohol, returned to blue, and stained with eosin, dehydrated, cleared with xylene, sealed with neutral gum, and observed under an optical microscope (Olympus, Tokyo, Japan).

Masson Collagen Staining

Paraffin sections were de-waxed, stained with hematoxylin less than 2 min, stained with Lichun magenta solution, and rapidly rinsed with 0.5% glacial acetic acid solution. Then the sections were stained with 1% aluminium phosphate aqueous solution, stained from dark red to bright red to pink, and observed under a microscope. Then the sections were stained with Aniline blue (Pulande), conventionally dehydrated with xylene and sealed. Medical Image analysis software Image-Proplus 6.0 was used to measure the positive staining area of collagenous fibers, and collagen volume fraction (CVF) = collagenous area/total field area. The staining location and color of collagenous fibers were distinguished (the cardiomyocytes

were red, and the collagenous fibers were blue banded or homogenous structures in the intercellular space).

Terminal Deoxynucleotidyl Transferase-Mediated Deoxyuridine Triphosphate-Biotin Nick End-Labeling (TUNEL) Staining

Paraffin sections were de-waxed, placed in the citrate buffer and baked at 350 W for 10 min. The sections were added with 50 μL TUNEL solution, joined with 50 μL conversion agent-peroxidase, developed with DAB, and observed under the microscope. The sections were put in hematoxylin, dipped with 95% ethanol I–II, joined with anhydrous ethanol I–II, xylene I–II, and sealed. The results were analyzed under an optical microscope.

Enzyme-Linked Immunosorbent Assay (ELISA)

Tumor necrosis factor α (TNF-α), interleukin (IL)-1β and IL-6 were detected by ELISA kits (BOSTER Biological Technology Co. Ltd., Wuhan, China). The eyeball blood was centrifuged at 604 g to collect the upper serum. The supernatant obtained by centrifugation from cell culture medium was detected in cell experiment. There were seven concentration gradients in the dilution standard of samples. The blank well was joined with sample diluent, and another well was added with tetramethylbenzidine (TMB), two duplicate wells were set for each concentration. The samples wells were joined with 50 μL of sample diluent and the samples in turn. Each well was reacted with 100 μL of primary antibody (except TMB well) for 1 h, as well as with 300 μL of 0.01 M tris-buffered saline (TBS) and 100 μL Avidin–Biotin-Peroxidase Complex working solution (except TMB well). Then each well was added with 300 μL of 0.01 M TBS and incubated with 100 μL TMB. The optical density (OD) value and the concentration of each well were immediately measured and the standard curve was drawn.

Reverse Transcription Quantitative Polymerase Chain Reaction (RT-qPCR)

MiR-133a, collagen I, collagen III, α-SMA, TGF-β1, CTGF, E-cadherin, and FSP-1 expression in myocardial tissues and cardiomyocytes were detected via RT-qPCR. The total RNA was extracted from cardiomyocytes or myocardial tissues and reversely transcribed to cDNA via RNA extraction kit (Takara, Dalian, China), and RT-PCR primers were synthesized via Invitrogen (Guangzhou, China), the sequences are shown in Table 1. Relative quantitative gene expression was analyzed by using glyceraldehyde-3-phosphate dehydrogenase (GAPDH) or U6 as the loading control genes according to $2^{-\triangle\triangle Ct}$ method.

Table 1 PCR primer sequence

Gene	Forward (5′–3′)	Reverse (5′–3′)
MiR-133a	TCATATTTGGTCCCCTTC AACC	TATCGTTGTTCTCCACTCCTT CAC
MAML1	AGCAACAGTTTCAGCGTCAT	GCACAGCAGCAGAAGGTC
Collagen I	GAGCGGAGAGTACTGGATCG	TACTCGAACGGGAATCCATC
Collagen III	TGGTCCTCAGGGTGTAAAGG	GTCCAGCATCACCTTTTGGT
α-SMA	ACTGGGACGACATGGAAA AG	CATCTCCAGAGTCCAGCACA
TGF-β1	CAGTGGCTGAACCAAGGA GA	GGAAGGGTCGGTTCATGTCA
E-cadherin	ATCTCCCTGGAAGCAGGATT	CGGGCTTTGCTGGTGATG
CTGF	ATCCCTGCGACCCACACAAG	CAACTGCTTTGGAAGGAC TCGC
FSP-1	ATGTAATAGTGTCCACCTTCC	ACTTCATTGTCCCTGTTGCT
GAPDH	TGCACCACCAACTGCTTAGC	GGCATGGACTGTGGTCATGAG
U6 snRNA	CTCGCTTCGGCAGCACA	AACCGCTTCACGAATTTGCGT

MiR-133a, MicroRNA-133a; MAML1, mastermind-like 1; GAPDH, glyceraldehyde-3-phosphate dehydrogenase; U6 snRNA; U6 small nuclear RNA

Western Blot Analysis

The rats were euthanized with anesthesia. The myocardial tissues were frozen and ground in liquid nitrogen. Then protease inhibitors phenylmethanesulfonylfluoride stock solution was mixed with cell lysis buffer at a ratio of 1:100 (Beyotime Biotechnology Co., Ltd., Shanghai, China). The samples were lysed with mixed solution and proteins of the cells were extracted. The total protein concentration was detected with the BCA kit. The samples were mixed with 5 × loading buffer at 4:1, implemented with boiling water bath for 10 min, ice-bathed, and centrifuged. Electrophoresis separation was performed, and the proteins were transferred to polyvinylidene fluoride (Servicebio) membrane with an electric transfer solution. Then the membrane was blocked with 5% skimmed milk powder, and joined with primary antibodies CD63, CD81, and CD9 (rabbit anti-rat polyclonal antibodies from Proteintech, 1:100), MAML1 (ab65090, Abcam, MA, USA, 1:1000), and GAPDH (Santa Cruz Biotechnology, Inc, Santa Cruz, CA, USA, 1:1000). Then the membrane was dripped with the secondary antibody, horseradish peroxidase-labeled IgG (Cell Signaling Technology, Beverly, MA, USA, 1:1000), and immersed in enhanced chemiluminescence reaction solution (Pierce, Rockford, IL, USA). With GAPDH as the loading control, protein imprinting images were analyzed with ImageJ2x software.

Cardiomyocyte Culture and Passage

SD rats aged 3–5 days (Experimental Animal Center of Zhejiang University School of Medicine, Zhejiang, China) were taken. The ventricular part was rinsed with precooled Hank's Balanced Salt Solution, cut into small pieces, and detached with 0.25% trypsin. The pieces were added with suitable amount of 10% complete medium for termination of detachment and centrifuged at 151 g. DMEM containing 20% FBS was applied for cell re-suspension. Cardiomyocytes were purified by differential adherent method, and the survival rate was observed via trypan blue staining, the survived cardiomyocytes were cultured. After 24 h, the cardiomyocytes adhered to the wall and began to pulse. After 72 h, the pseudopodia expanded.

Construction of VMC Model of Cardiomyocyte

Cardiomyocytes in the 4th passage in the logarithmic growth phase were selected and infected with MSC^{Exo}, NC^{Exo}, Adas-miR-133a^{Exo}, and Ad-miR-133a^{Exo}. The 100 Tcid50 CVB3 virus solution (100 μL) was added into the cells to induce a cell VMC model. At the same time, equal amount of maintenance solution was added to the cells for a control, and corresponding exosomes were joined into cardiomyocytes after 1-h infection for 47-h culture.

Cell Counting Kit (CCK)-8 Assay

CCK-8 cell detection kit (Beyotime) was applied to detect the survival rate of cardiomyocytes. When growing to logarithmic phase, the cells were detached with 0.25% trypsin, and seeded into 96 well cell culture plate at 2.5×10^4 cells/per well. Joined with CCK-8 solution (10 μL/well), cells were continually cultured for 1–4 h, and the $OD_{450\ nm}$ value was measured via a microplate reader.

Flow Cytometry

AnnexinV-APC/propidium iodide (PI) double staining method was applied to detect cell apoptosis. The cells were centrifuged, re-suspended with 250 μL Binding Buffer (4 mL Binding Buffer + 12 mL deionized water), and adjusted to 1×10^6 cells/mL. The 100 μL cell suspension was added with 5 μL Annexin V-APC (BD Biosciences) and 5 μL PI solution (BD Biosciences), loaded on the flow cytometer, and analyzed automatically by a computer.

Dual Luciferase Reporter Gene Assay

The wild-type (wt) or mutant-type (mut) sequence of MAML1 3-untranslated region (UTR) was cloned into pGL3-M vector (Promega, WI, USA), then MAML1-3-UTR-wt or MAML1-3-UTR-mut were generated. The vectors, together with miR-133a mimic or NC, were co-transfected into cardiomyocytes via Lipofectamine 2000. The luciferase activity was tested 48 h later by the dual luciferase reporter gene system (Promega) [21]

RNA Immunoprecipitation (RIP) Assay

RIP kit (Millipore, USA) was used to detect the binding of MAML1 and miR-133a. Cells were lysed by radioimmunoprecipitation assay buffer (P0013B, Beyotime, Shanghai, China), centrifuged at 1400 g and incubated with antibodies to co-precipitate. Magnetic beads (50 μL) were resuspended in 100 μL RIP Wash Buffer and incubated with 5 g anti-MAML1 antibody (1 g/mL, ab155786) or IgG (1:100, ab172730). The magnetic bead-antibody complex was resuspended in 900 μL RIP Wash Buffer, interacted with 100 μL cell extract, digested with proteinase K, and detected by RT-qPCR [22].

Statistical Analysis

SPSS 21.0 statistical software (IBM Corp. Armonk, NY, USA) was applied for analysis of the data. The measurement data were expressed as mean ± standard deviation. The t test was applied to comparisons between two groups. One-way analysis of variance (ANOVA) was used for comparison among groups, and Tukey's post hoc test for pairwise comparisons. Predictors were kept if they were significant at a P value of 0.05 or smaller.

Results

Identification of BMSCs and BMSC-Exo

Microscopically, BMSCs were fusiform and rounded, and adhered to the wall in a vortex or radial pattern (Fig. 1A). After oil red O staining of adipogenesis induction, the lipid droplets of the 4th BMSCs were red, and there were round lipid droplets of different sizes (Fig. 1B). After induction of osteogenesis, the cells expressing calcified nodules showed red after alizarin red staining, and uneven distribution of calcified nodules and overlapping cells (Fig. 1C). Flow cytometry manifested that the MSC markers CD29 and CD44 (> 95%) were expressed, but the hematopoietic stem cell surface antigen CD34 (< 95%) was not expressed (Fig. 1D). These results manifested that the BMSCs were of high purity and conformed to MSC standards of International Society of Cell Therapy.

Transmission electron microscope observed that BMSC-Exos were oval vesicles with clear peripheral membranous structure, different sizes, and a diameter of 40–100 nm (Fig. 1E). Western blot analysis demonstrated that the extracted products expressed exosome originated characteristic proteins of CD9, CD63, and CD81 (Fig. 1F).

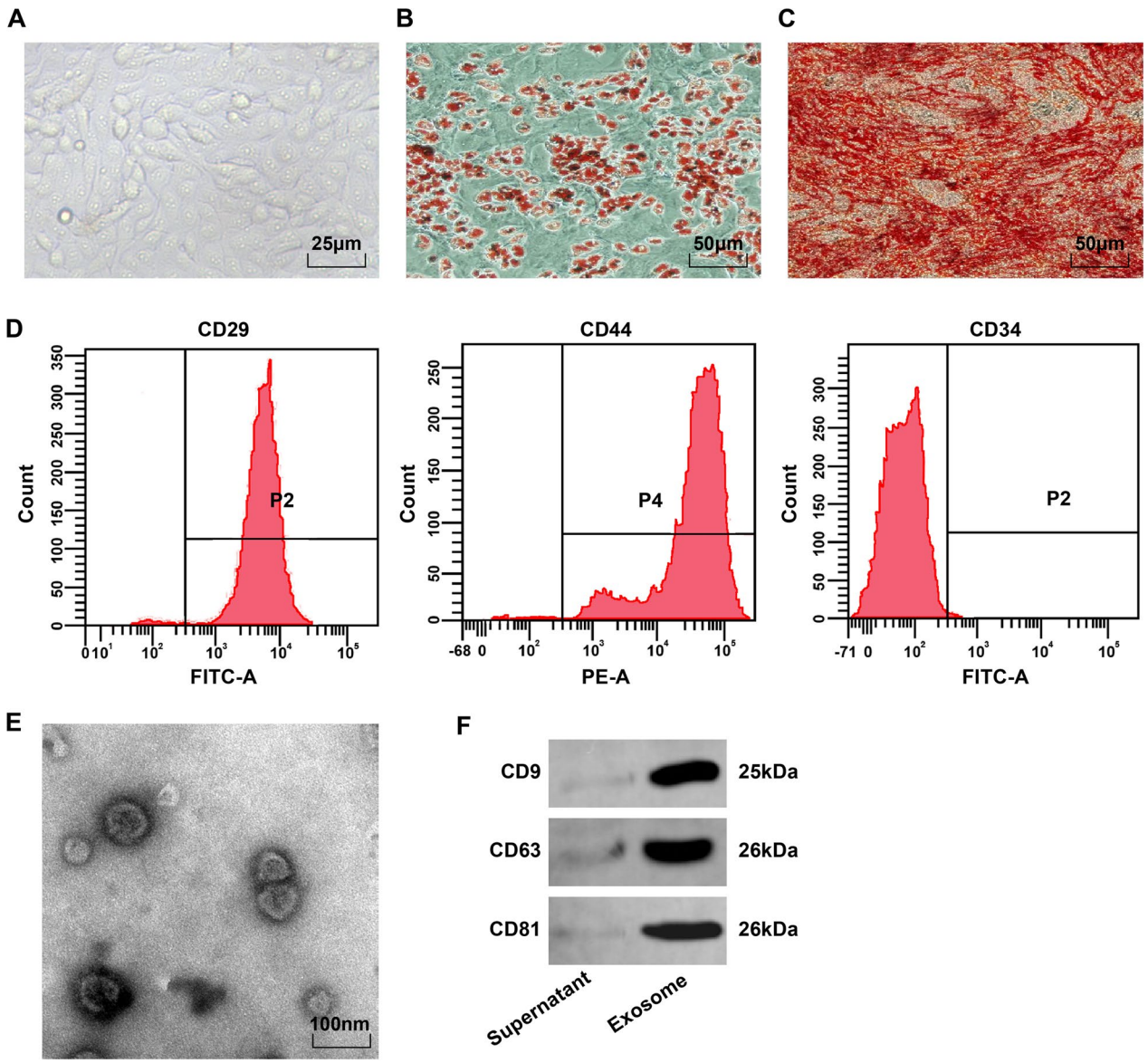

Fig. 1 BMSC phenotype observation and BMSC-Exo identification. **A** Morphological observation of BMSCs in the 4th passage; **B** The results of oil red O staining of adipocytes; **C** The results of alizarin red staining of osteoblasts; **D** The phenotype of BMSC detected via flow cytometry. **E** Electron microscope observation of BMSC-Exo; **F** Protein bands of CD9, CD63, and CD81

Elevated Exosomal miR-133a Improves the Symptoms of Myocarditis

The transfection of BMSCs with miR-133a recombinant adenovirus was observed (Fig. 2A). A large number of green fluorescence expression of NC, Ad-miR-133a, and Adas-miR-133a were observed under the inverted fluorescence microscope, indicating that recombinant adenovirus vector could effectively transfect BMSCs. To test the transfection efficiency of miR-133a, miR-133a expression in BMSCs and their exosomes was measured by RT-qPCR. It was discovered that miR-133a up-regulation increased miR-133a expression while miR-133a down-regulation decreased miR-133a expression (Fig. 2B). Subsequently, we injected exosomes containing miR-133a in rats. Under the inverted fluorescence microscope, green fluorescence expression was observed in VMC rats after treatment of NC^{Exo}, Ad-miR-133a^{Exo}, or Adas-miR-133a^{Exo}, indicating that the recombinant adenovirus vector infected myocardial tissues of rats (Fig. 2C). RT-qPCR experiment also found that miR-133a expression in VMC rats was apparently decreased; miR-133a expression was

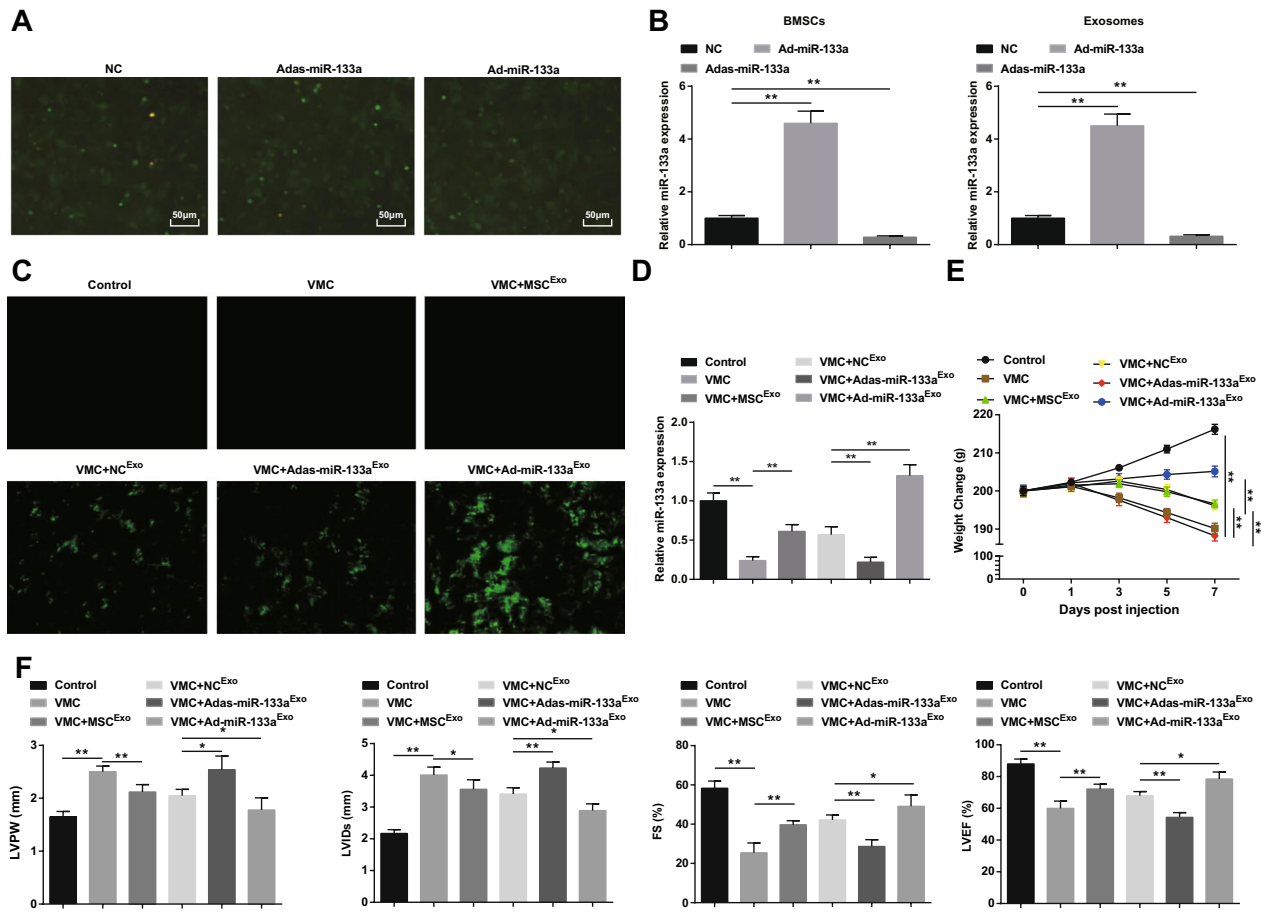

Fig. 2 Up-regulated exosomal miR-133a alleviates myocarditis. **A** BMSCs transfection of miR-133a recombinant adenovirus; **B** RT-qPCR detection of miR-133a expression in BMSCs and their exosomes after regulating miR-133a; **C** miR-133a transfection efficiency tested via inverted fluorescence microscope; **D** The relative expression of miR-133a in myocardial tissues tested via RT-qPCR; **E** Weight change of rats in each group; **F** Determination of LVPW, LVIDs, FS and LVEF in rats of each group. $^{*}P < 0.05$; $^{**}P < 0.001$

obviously elevated in VMC rats injected with Ad-miR-133a^{Exo} but decreased in VMC rats injected with Adas-miR-133a^{Exo} (Fig. 2D). As to the general conditions of rats, it was observed that the general conditions of normal control rats were normal, and the characteristics of VMC were apparently expressed in VMC rats and VMC rats injected with Adas-miR-133a^{Exo}, such as rough and disorderly hair, dyspnea, and little diet. In VMC rats treated with MSC^{Exo}, NC^{Exo}, and Ad-miR-133a^{Exo}, these signs were improved to different degrees. The weight of the VMC rats was continually decreased from 1 days after infection, and injection of MSC^{Exo}, NC^{Exo}, or Ad-miR-133a^{Exo} increased the weight of rats. The weight of the VMC rats treated with Ad-miR-133a^{Exo} was increased obviously and the weight of the VMC rats injected with Adas-miR-133a^{Exo} was clearly decreased (Fig. 2E).

The myocardial function observation suggested that (Fig. 2F), the VMC rats had increased LVPW and LVIDs, and decreased FS and LVEF. After exosome injection, declined LVPW and LVIDs, and obviously elevated FS and LVEF showed in VMC rats. Adas-miR-133a^{Exo} treatment impaired while Ad-miR-133a^{Exo} improved myocardial function in VMC rats.

Up-regulated Exosomal miR-133a Inhibits Inflammation in Myocardial Tissues of VMC Rats

HE staining manifested that the myocardial fibers in normal control rats were closely arranged and there was no inflammatory cell infiltration in the mesenchyme. The cardiomyocytes in the VMC rats were disorganized and the mesenchyme was infiltrated by a large number of inflammatory cells. The cardiomyocytes in VMC rats injected with MSC^{Exo} or NC^{Exo} were orderly arranged,

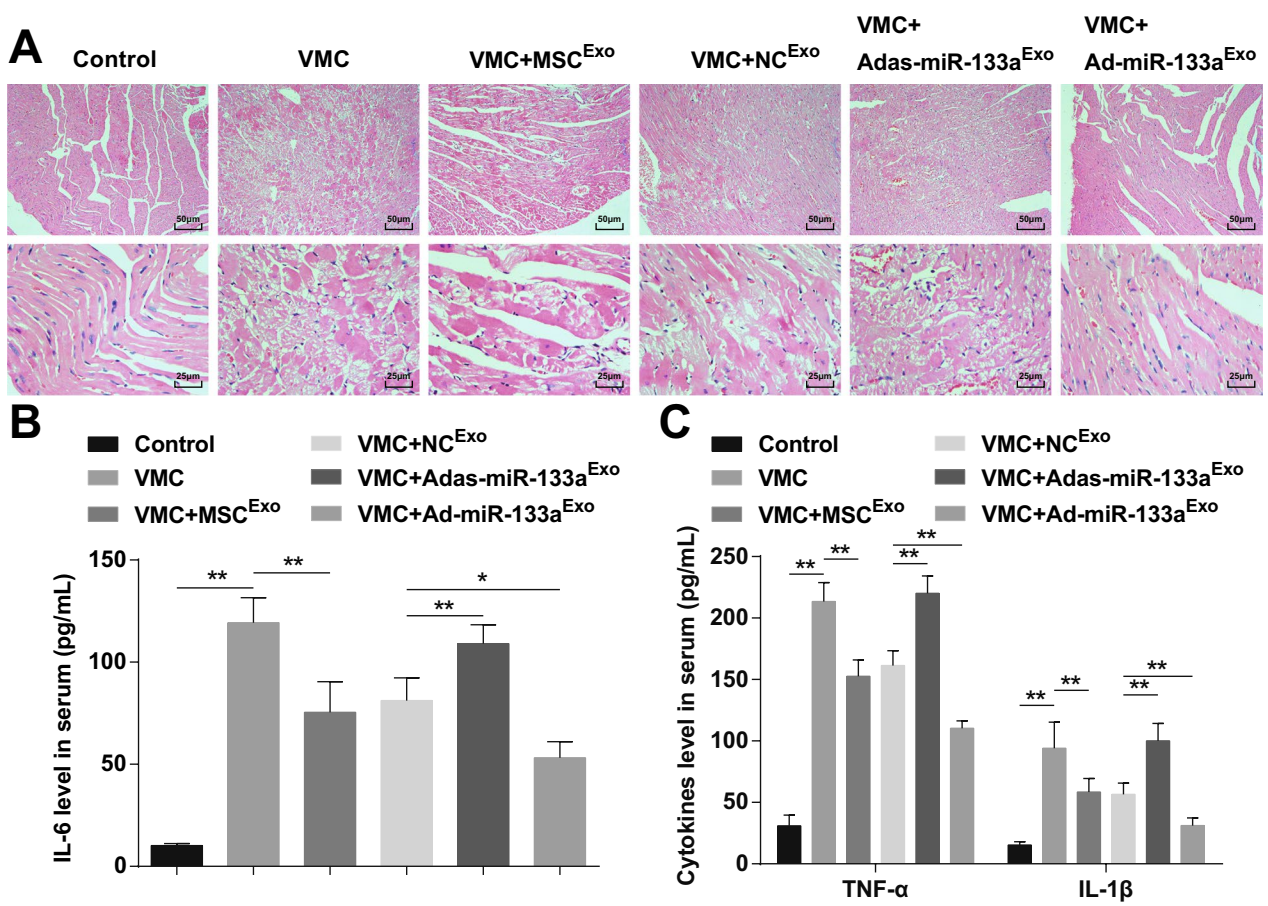

Fig. 3 Increased exosomal miR-133a restrains inflammation in myocardial tissues with VMC. **A** HE staining of rat myocardial tissue in each group; **B** The expression of IL-6 in serum tested via ELISA; **C** The expression of TNF-α and IL-1β in serum tested via ELISA. *$P < 0.05$; **$P < 0.001$

with a small amount of inflammatory cells infiltrating in the mesenchyme. The cardiomyocytes in VMC rats after Adas-miR-133a^{Exo} treatment were disorderly arranged, and the inflammatory cells in the mesenchyme were infiltrated. The cardiomyocytes in VMC rats treated with Ad-miR-133a^{Exo} were orderly arranged without obvious inflammatory cells infiltration (Fig. 3A).

ELISA indicated that (Fig. 3B, C) inflammatory factors (TNF-α, IL-1β, and IL-6) were obviously increased in VMC rats. The VMC rats injected with Ad-miR-133a^{Exo} had reduced levels of inflammatory factors. Adas-miR-133a^{Exo} treatment caused elevated inflammatory factors in VMC rats.

Elevated Exosomal miR-133a Decreases CVF in Myocardial Tissues of Rats with VMC

Masson staining disclosed that the myocardial fibers in normal rats were closely arranged, with almost no blue collagenous fibers. After CVB3 injection, the cardiomyocytes were hypertrophic, with connective tissue hyperplasia and a large number of blue collagenous fibers, and CVF was obviously elevated. Treated with exosomes, the cardiomyocytes were orderly arranged, intercellular connective tissue hyperplasia was decreased, blue collagen fibers and CVF were clearly decreased. The myocardial intercellular space of VMC rats injected with Adas-miR-133a^{Exo} was widened, the cells were obviously enlarged, the blue collagen fibers and CVF were clearly increased; the intercellular space was decreased, the distribution of blue collagen fibers and the CVF were decreased of VMC rats with Ad-miR-133a^{Exo} treatment (Fig. 4A, B).

Increased Exosomal miR-133a Reduces the Expression of Collagen I, Collagen III, TGF-β1, and CTGF in Myocardial Tissues of Rats with VMC

Collagen I and collagen III are the main components of collagen, which are mainly distributed in cell junctions and cell membranes, intercellular substance, and cytoplasm. TGF-β1 and CTGF are the hallmark proteins of fibrosis. Findings of RT-qPCR demonstrated that collagen I, collagen III, TGF-β1, and CTGF mRNA expression levels were increased in VMC rats, but decreased after

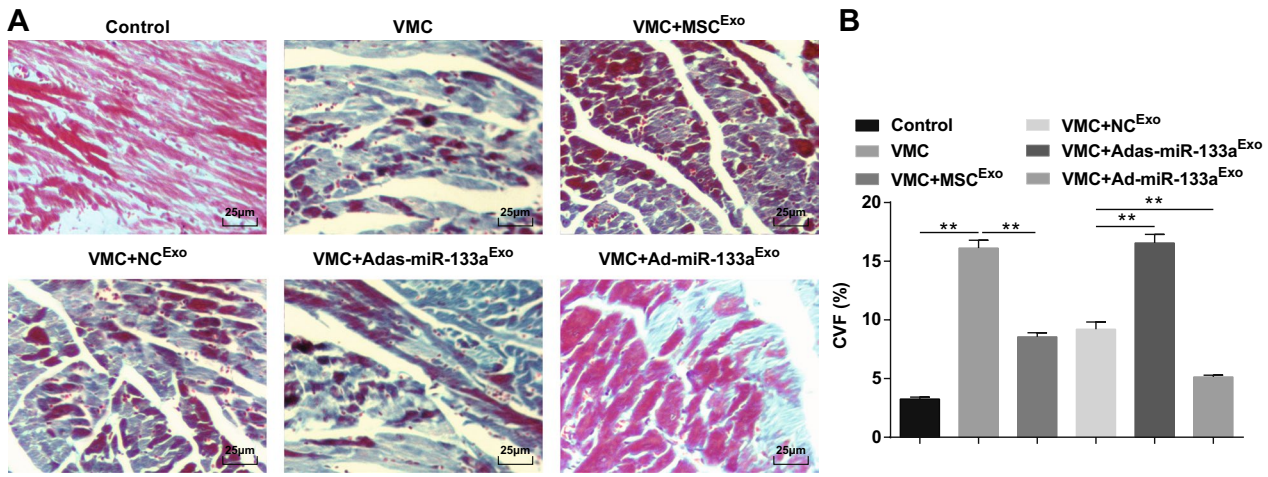

Fig. 4 Up-regulated exosomal miR-133a decreases CVF in myocardial tissues of rats with VMC. **A** Masson staining of myocardial tissues in rats; **B** Collagen volume fraction of rats in each group. $^{**}P < 0.001$

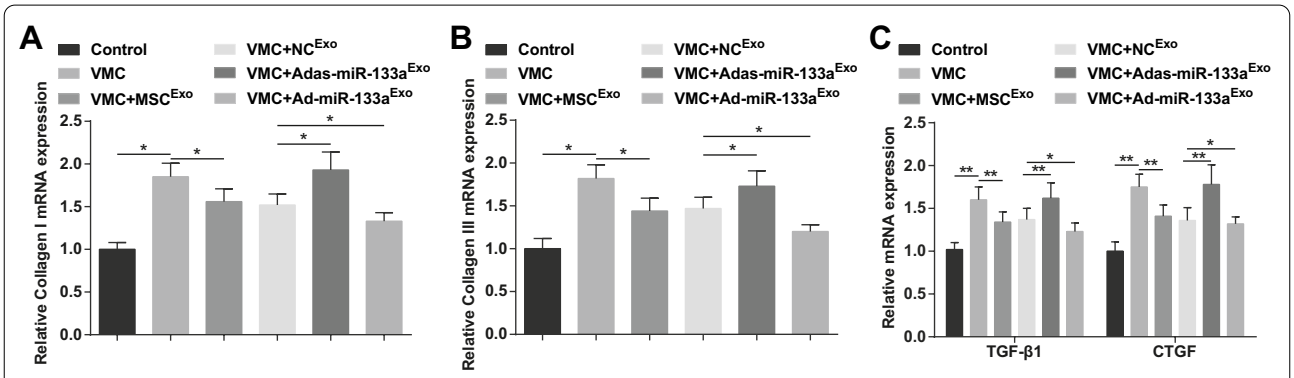

Fig. 5 Elevated exosomal miR-133a reduces the mRNA expression of collagen I, collagen III, TGF-β1 and CTGF in myocardial tissues of rats with VMC. **A** Collagen I mRNA expression in myocardial tissues of rats was detected by RT-qPCR; **B** Collagen III mRNA expression in myocardial tissues of rats was detected by RT-qPCR; **C** TGF-β1 and CTGF mRNA expression in myocardial tissues of rats was detected by RT-qPCR. $^{*}P < 0.05$; $^{**}P < 0.001$

exosome treatment. The VMC rats treated with Ad-miR-133a^{Exo} had decreased mRNA expression levels of collagen I, collagen III, TGF-β1, and CTGF while the VMC rats after Adas-miR-133a^{Exo} treatment showed the opposite situation (Fig. 5A–C).

Up-regulated Exosomal miR-133a Inhibits the Cardiomyocyte Apoptosis in Myocardial Tissues of Rats with VMC

TUNEL staining showed that the apoptotic cardiomyocytes were brownish black or brownish yellow with nuclear condensation. The number of apoptotic cells was increased in VMC rats which would be attenuated by exosome treatment. The VMC rats injected with Ad-miR-133a^{Exo} had reduced number of apoptotic cells and those injected with Adas-miR-133a^{Exo} had increased number of apoptotic cells (Fig. 6A, B).

Elevated Exosomal miR-133a Depresses EMT in Myocardial Tissues of Rats with VMC

E-cadherin, α-SMA, and FSP-1 are key indicators of EMT. Results of RT-qPCR demonstrated that α-SMA and FSP-1 mRNA expression levels were elevated and E-cadherin mRNA expression level was decreased in VMC rats. In addition, α-SMA and FSP-1 mRNA expression levels were reduced and E-cadherin mRNA expression level was increased in VMC rats after exosome treatment. α-SMA and FSP-1 mRNA expression levels were elevated and E-cadherin mRNA expression level was decreased in VMC rats treated with Adas-miR-133a^{Exo},

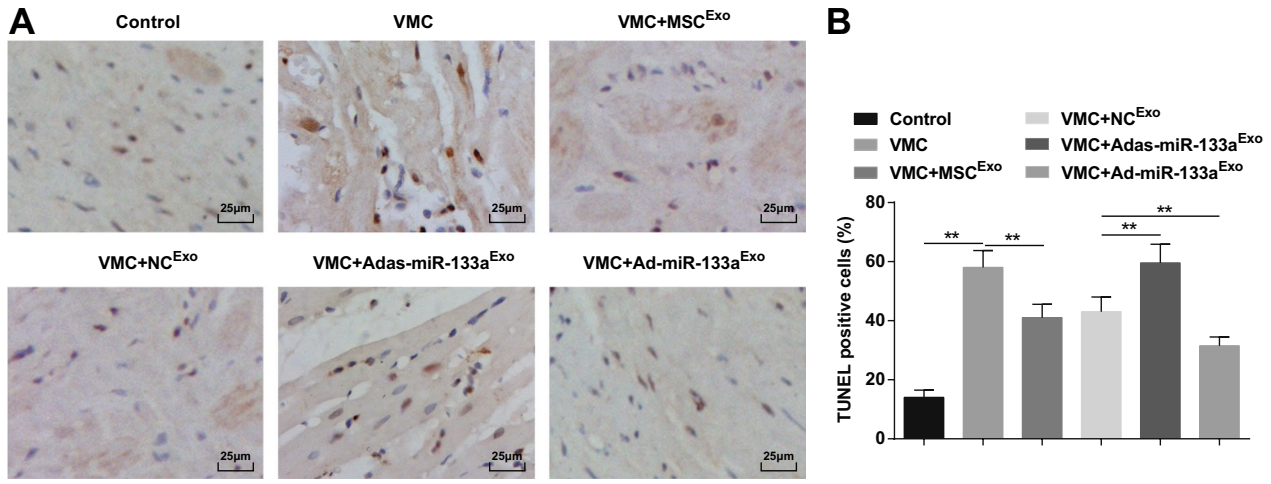

Fig. 6 Increased exosomal miR-133a inhibits the cardiomyocyte apoptosis in myocardial tissues of rats with VMC. **A** TUNEL staining of rat myocardial tissues in each group; **B** The number of TUNEL positive cells in each group. $^{**}P < 0.001$

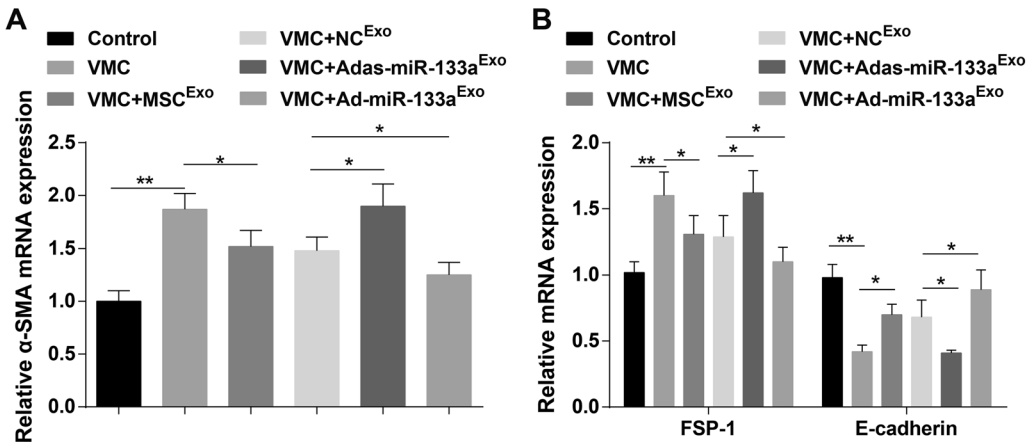

Fig. 7 Up-regulated exosomal miR-133a represses EMT in myocardial tissues of rats with VMC. **A** The mRNA expression of α-SMA in rat myocardial tissues in each group was detected by RT-qPCR; **B** The mRNA expression of FSP-1 and E-cadherin in rat myocardial tissues in each group was detected by RT-qPCR. $^{*}P < 0.05$; $^{**}P < 0.001$

while the expression of these indicators was opposite in VMC rats injected with Ad-miR-133a^{Exo} (Fig. 7A, B).

Up-regulated Exosomal miR-133a Depresses Inflammation of Cardiomyocytes in VMC

As a result, fluorescence microscopy captured green fluorescent expression in VMC rats treated with NC^{Exo}, Ad-miR-133a^{Exo}, or Adas-miR-133a^{Exo}, indicating that the recombinant adenovirus vector infected cardiomyocytes of rats (Fig. 8A). RT-qPCR and ELISA discovered that (Fig. 8B, D) miR-133a expression was reduced and inflammatory factors (TNF-α, IL-1β, and IL-6) were increased in VMC rats, which would be reversed by exosome treatment. The VMC rats treated with Ad-miR-133a^{Exo} had up-regulated miR-133a and decreased inflammatory factors in VMC rats, while those treated with Adas-miR-133a^{Exo} presented decreased miR-133a and increased levels of inflammatory factors in VMC rats.

Elevated Exosomal miR-133a Promotes Cell Viability, and Represses Apoptosis of Cardiomyocytes in VMC

The apoptosis and the cell viability were detected via AnnexinV-APC/PI double staining and CCK-8 assay. The results revealed that there was an obvious increase in apoptosis rate, a decrease in cell viability

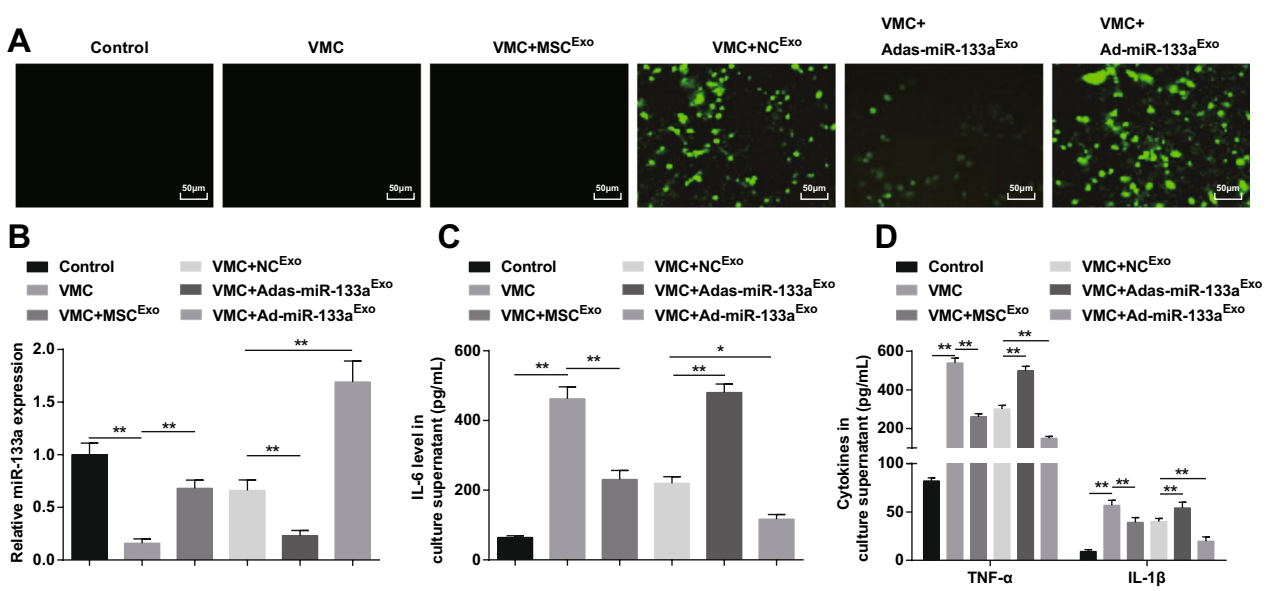

Fig. 8 Elevated exosomal miR-133a restrains inflammation of cardiomyocytes in VMC. **A** miR-133a transfection efficiency tested via inverted fluorescence microscope; **B** The relative expression of miR-133a in cardiomyocytes of rats in each group; **C** IL-6 expression in culture supernatant of cardiomyocytes in each group; **D** TNF-α and IL-1β expression in culture supernatant of cardiomyocytes in each group. *$P < 0.05$; **$P < 0.001$

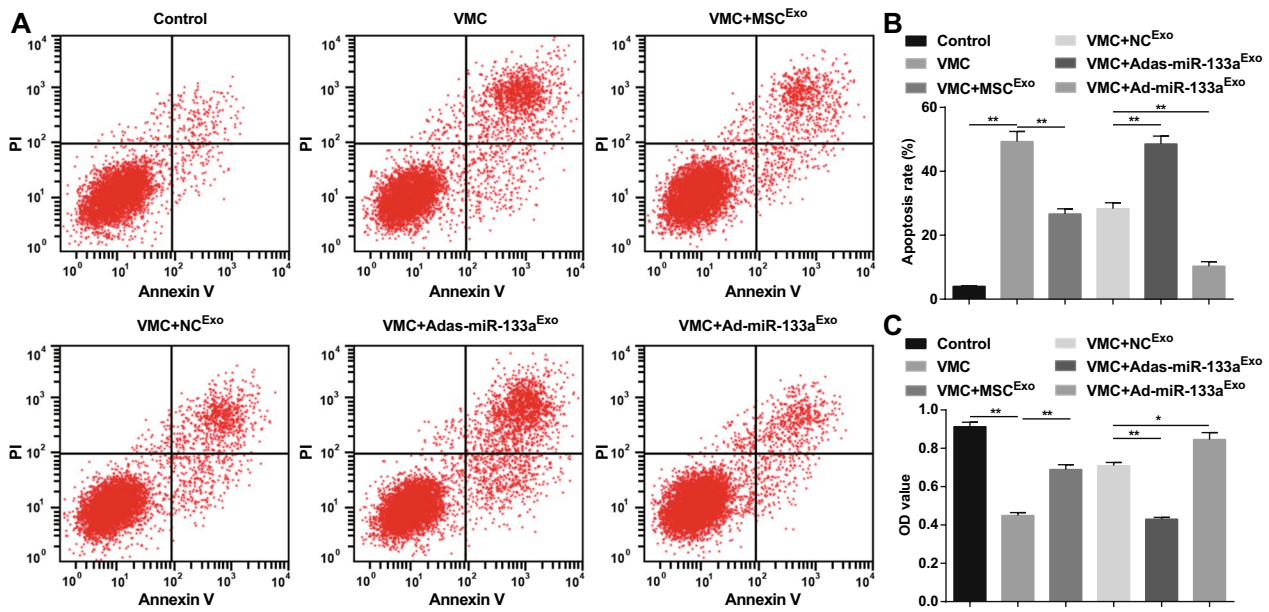

Fig. 9 Increased exosomal miR-133a promotes viability and represses apoptosis in cardiomyocytes in VMC. **A** The cardiomyocytes apoptosis detected via flow cytometry; **B** Quantification results of A; **C** The cell viability detected via CCK-8 assay. *$P < 0.05$; **$P < 0.001$

of cardiomyocytes in VMC rats. Exosome treatment reduced apoptosis rate and enhanced the viability of cardiomyocytes. Adas-miR-133a^{Exo} enhanced the apoptosis rate and disrupted the viability of cardiomyocytes in VMC rats. Ad-miR-133a^{Exo} treatment functioned the opposite effects on cardiomyocytes of VMC rats (Fig. 9A–C).

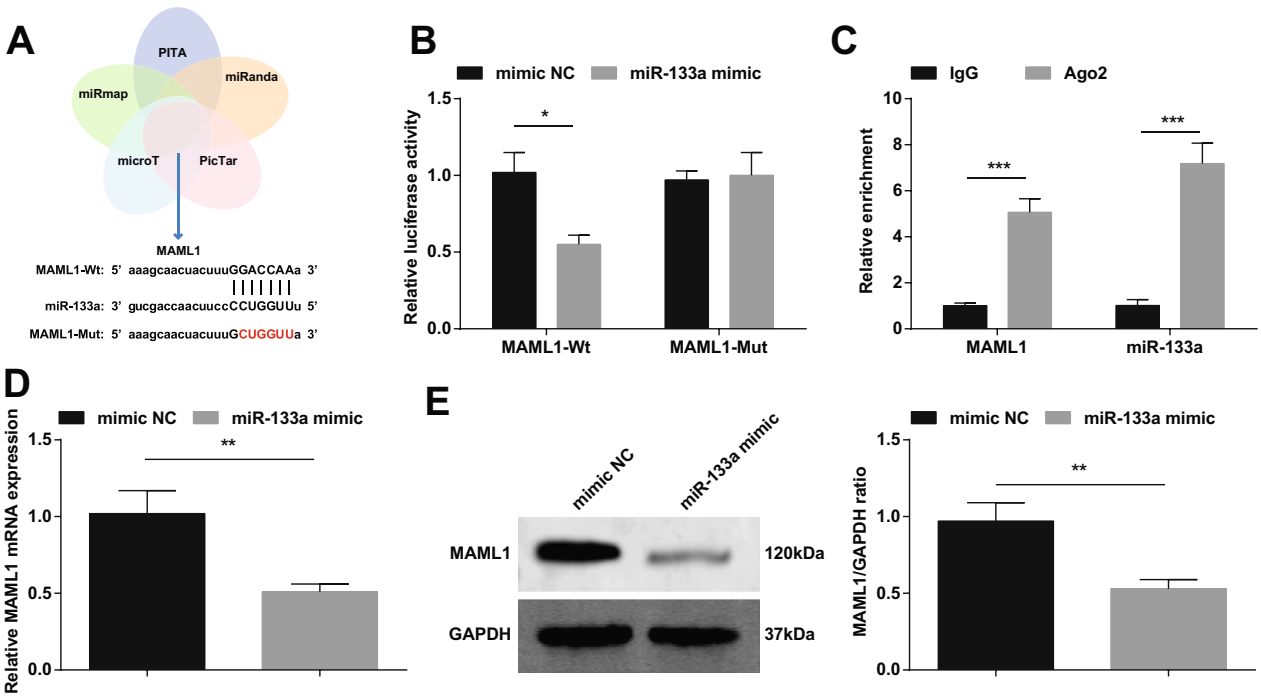

Fig. 10 miR-133a targets MAML1. **A** miR-133a's targets predicted on bioinformatics websites; **B** The targeting relationship between miR-133a and MAML1 verified by dual luciferase reporter gene experiment; **C** The targeting relationship between miR-133a and MAML1 verified by RIP experiment; **D**/**E** MAML1 expression changes after up-regulation of miR-133a detected by RT-qPCR and Western blot. **P* < 0.05; ***P* < 0.01; ****P* < 0.001

miR-133a Targets MAML1

It has been reported that up-regulated miRNA-193b reduces myocardial I/R damage by targeting MAML1 [18]. Based on that, we cross-screened downstream genes of miR-133a through bioinformatics websites PITA, miRanda, PicTar, microT and miRmap, and selected MAML1 as a target of miR-133a (Fig. 10A). We constructed MAML1-wt or MAML1-mut, and co-transfected cardiomyocytes with miR-133a mimic or NC. The results showed that miR-133a mimic reduced the luciferase activity of MAML1-wt (Fig. 10B). The RIP experiment further verified the targeting relationship between miR-133a and MAML1 (Fig. 10C). RT-qPCR and Western blot detection of MAML1 expression showed that MAML1 expression was decreased in cardiomyocytes transfected with miR-133a mimic (Fig. 10D, E).

Inhibition of MAML1 has a Protective Effect on Rats with Myocarditis and Reverses the Effect of miR-133a-Inhibited Exosomes on Rats with VMC

To further study the effect of miR-133a-regulated MAML1 on rats with VMC, we injected si-MAML1 or si-NC adenovirus into VMC rats or VMC rats that had been treated with miR-133a-silenced exosomes. The injection success was validated by RT-qPCR and Western blot (Fig. 11A, B). The results manifested that injection of si-MAML1, the weight of VMC rats was increased (Fig. 11C), cardiac function was improved (Fig. 11D–G), myocardial tissue pathology and fibrosis were attenuated (Fig. 12A–C), serum inflammation (Fig. 12D, E) and cardiomyocyte apoptosis (Fig. 13A–G) were inhibited. Also, the deleterious effects of miR-133a-silenced exosomes in VMC rats were reversed after injection of si-MAML1.

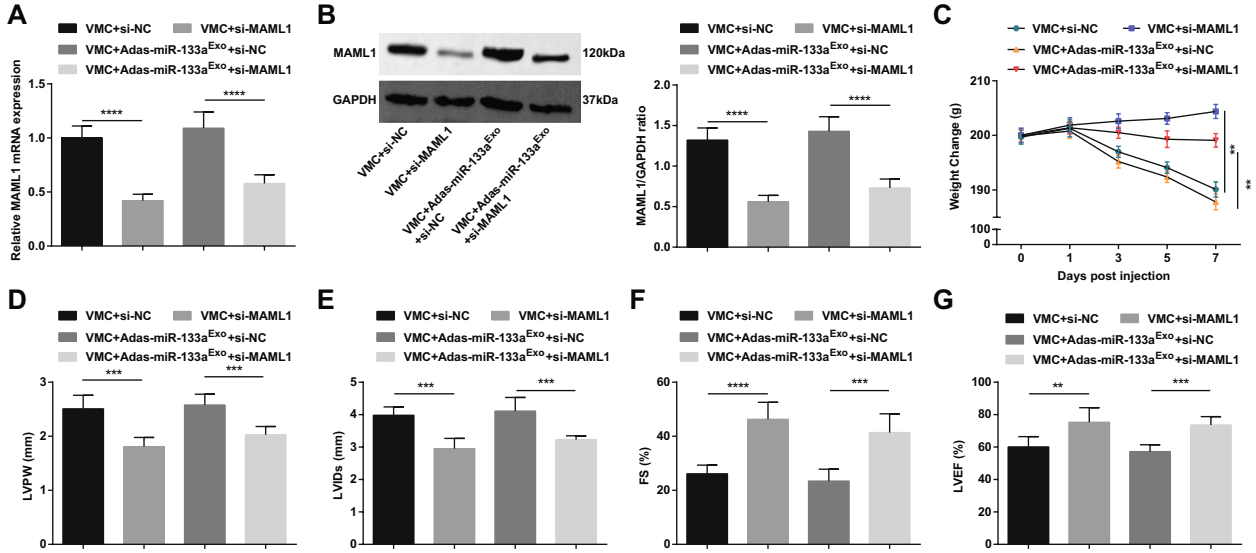

Fig. 11 Inhibition of MAML1 has a protective effect on myocarditis rats and can reverse the effect of miR-133a-silenced exosomes on rats with VMC. **A**/**B** MAML1 expression in myocardial tissue of rats detected by RT-qPCR and Western blot; C. Weight change of rats; **D**–**G** Determination of LVPW, LVIDs, FS and LVEF in rats; $^{**}P < 0.01$; $^{***}P < 0.001$; $^{****}P < 0.0001$

Discussion

Myocarditis is an inflammatory heart illness resulting in DCM and heart failure and is most frequently induced by viral infections such as CVB3 [2]. A study has revealed that miR-133 relieves cardiomyocyte apoptosis and electrical remodeling in mice with VMC [23]. Additionally, changed exosomal miRNAs are also found to be linked with the pathogenesis of CVB3-induced myocarditis [14]. Exosomes derived from cardiac progenitor cells ease CVB3-induced apoptosis via restraining the proliferation of CVB3 in VMC [24]. This study explored the regulatory mechanism of BMSC-derived exosomal miR-133 on myocardial fibrosis and EMT in VMC rats (Additional file 1: Fig. 1).

The study found that the expression of miR-133a was decreased in VMC. As demonstrated before, miR-133a expression is decreased in MI [7]. A study has also suggested that the relative expression of miR-133 in mouse hearts of the VMC is obviously decreased with contrast to the controls [23]. There are some connections of miRNAs with exosomes. The differential expression of exosomes and of exosomal miRNAs in illness has been regarded as biomarkers of disease with performance of noninvasive clinical diagnosis together with their therapeutic potentials [25]. Lin et al. have found that miR-133 is specially sorted into hypoxia/reoxygenation (H/R)-caused human endothelial progenitor cells-derived exosomes to increase fibroblast angiogenesis and EMT [26]. Another study has revealed that MSCs exhibits a communication with brain parenchymal cells and may modulate neurite outgrowth by transfer of miR-133b to neural cells via exosomes [27].

The major finding of this work manifested that up-regulated exosomal miR-133a promoted cell viability, inhibited inflammation, apoptosis, EMT, and fibrosis in rats with VMC. They suits well with a former research that miR-133a silence reverses the *Astragalus polysaccharides* treatment-induced osteosarcoma MG63 cell proliferation inhibition, together with cell apoptosis promotion [28]. Another study has revealed that overexpressed miR-133a suppresses angiogenesis, apoptosis, fibrosis, and inflammation, while accelerating therapeutic cardiac remodeling in ischemic myocardial illnesses [29]. Similar to our study, Li et al. have stated that miR-133 inhibits cardiomyocyte apoptosis by regulating the expression of apoptosis-related genes in the hearts of VMC mice [23]. The over-expressed miR-133a has been reported to depress hypoxia-induced apoptosis and strengthen cardiomyocyte survival [30]. Meanwhile, the up-regulated serum exosomal miR-30a and miR-181d may have the potentials to be applied as biomarkers for VMC diagnosis [14].

Another finding in our study was that up-regulated exosomal miR-133a decreased CVF, reduced the expression of collagen I and collagen III in rats with VMC. A article has elucidated that released fibroblast growth factor-18 from a collagen membrane causes osteoblastic activity participating in down-regulated miR-133a [31]. In vitro excessive expression of miR-133a depresses cardiomyocyte hypertrophy

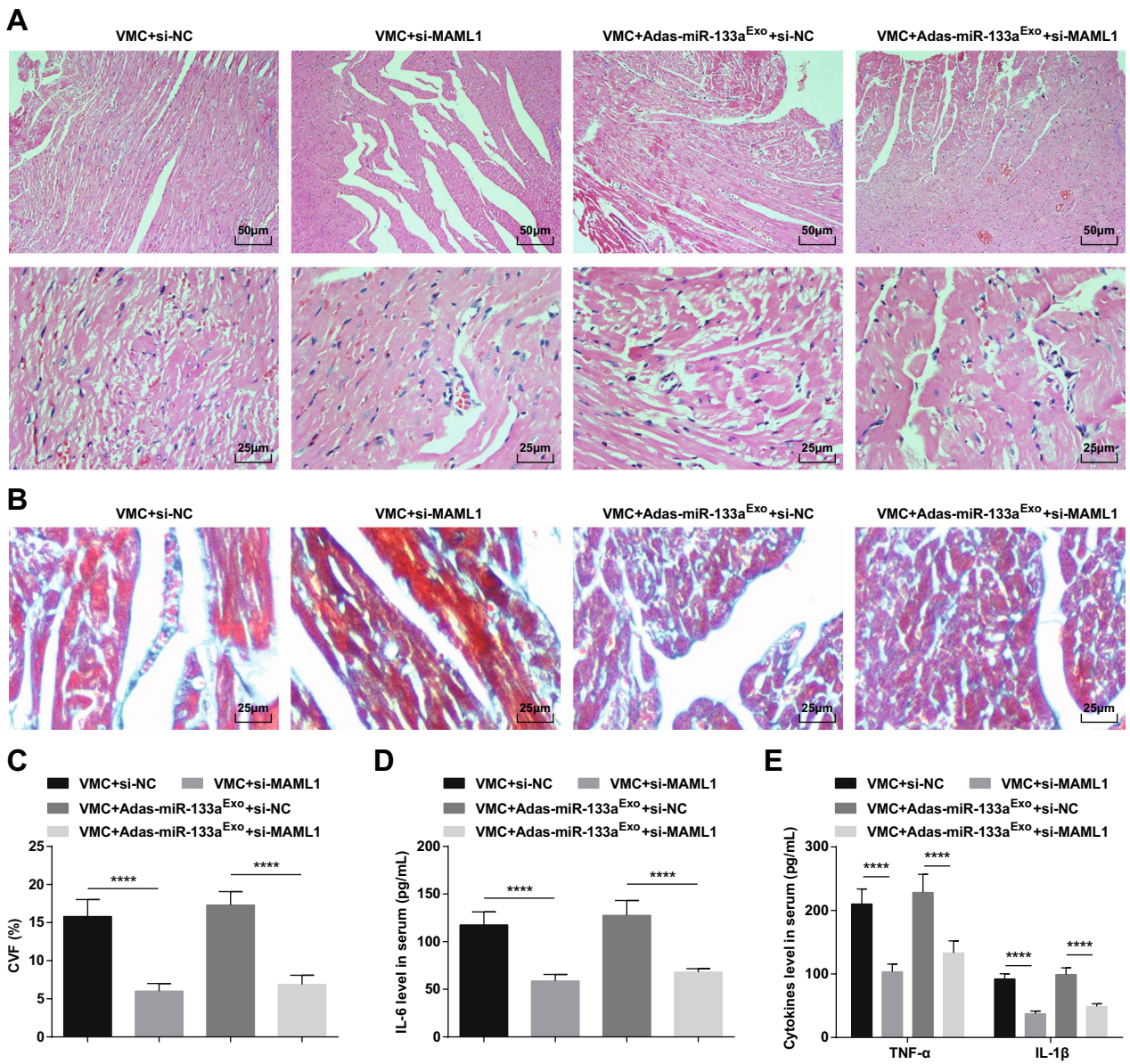

Fig. 12 Inhibition of MAML1 can reverse the effect of miR-133a-silenced exosomes on rats with VMC. **A** HE staining of rat myocardial tissue; **B** Masson staining of myocardial tissues in rats; **C** CVF of rats; **D** The expression of IL-6 in serum tested via ELISA; **E** The expression of TNF-α and IL-1β in serum tested via ELISA.****$P < 0.0001$

and reduces collagen expression [32], as evidenced in another study. CVF equals the ratio of collagen area to the sum of myocardial area and collagen area, and the mean value shows the CVF of the section [33]. This finding is also reported by Wang et al. that VMC mice model is successfully constructed by CVB3 infection, manifesting apparent higher CVF expression in contrast with the control group [34]. Moreover, the finding is consistent with that of Ferreira et al. who demonstrates that miR-133a may take on a major role in the modulation of gene expression in chronic Chagas disease cardiomyopathy pathogenesis, with potential link as diagnostic and prognostic tools [8]. Furthermore, evidence has shown that knocking down MAML1 can reduce the hypertrophy of pre-treated cardiomyocytes [35]. In our study, we found that MAML1 was the target gene of miR-133a and inhibition of MAML1 reversed

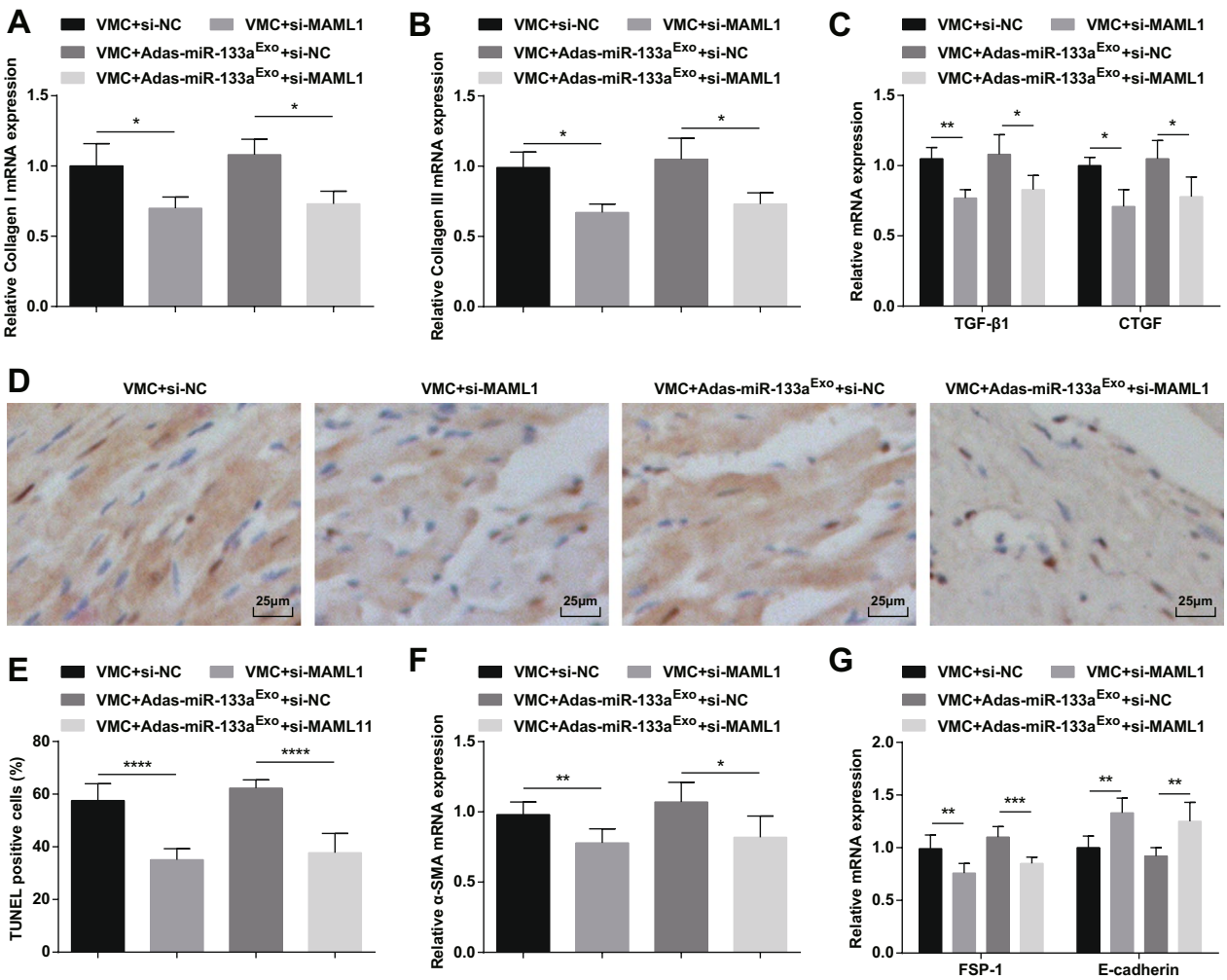

Fig. 13 Inhibition of MAML1 can reverse the effect of miR-133a-inhibiting exosomes on rats with VMC. **A** Collagen I mRNA expression in myocardial tissues of rats was detected by RT-qPCR; **B** Collagen III mRNA expression in myocardial tissues of rats was detected by RT-qPCR; **C** TGF-β1 and CTGF mRNA expression in myocardial tissues of rats was detected by RT-qPCR; **D** TUNEL staining of rat myocardial tissues in each group; **E** The number of TUNEL positive cells in each group. **F** The mRNA expression of α-SMA in rat myocardial tissues in each group was detected by RT-qPCR; **G** The mRNA expression of FSP-1 and E-cadherin in rat myocardial tissues in each group was detected by RT-qPCR. *$P < 0.05$; **$P < 0.01$; ****$P < 0.0001$

the effects of miR-133a-silenced exosomes on rats with VMC. In myocardial ischemia–reperfusion injury, miR-193b-mediated down-regulation of MAML1 could in part reduce infarction and myocardial enzymes, as well as attenuate apoptosis of cardiomyocytes [18]. Also, there is a report suggesting that deficiency of MAML1 could relieve hepatic fibrogenesis [19].

Conclusion

In conclusion, this present study offers evidence that miR-133a is down-regulated in rats with VMC, and elevated exosomal miR-133a improves cardiac function and restrains myocardial fibrosis and EMT in rats with VMC, as well as enhances viability and represses apoptosis of cardiomyocytes in VMC through targeting MAML1. Our study also suggests that inhibition of MAML1 has a protective effect on rats with myocarditis and reverses the effect of miR-133a-inhibited exosomes on rats with VMC. The identification of the exosomal miR-133a in myocardial fibrosis and EMT of myocarditis may potentially widen our understanding of mechanisms underpinning myocarditis and also bear clinical value as a novel molecular target. More researches should be undertaken for making inroads into the treatment of this disease.

Abbreviations
miR-133: MicroRNA-133; BMSC-Exo: Bone marrow mesenchymal stem cell-derived exosome; EMT: Epithelial–mesenchymal transition; VMC: Viral myocarditis; CVF: Collagen volume fraction; DCM: Dilated cardiomyopathy; CVB3: Coxsackie B3 virus; miRNAs: MicroRNAs; MI: Myocardial infarction; SPF: Specific pathogen-free; SD: Sprague–Dawley; DMEM: Dulbecco's Modified Eagle Medium; PBS: Phosphate-buffered saline; FBS: Fetal bovine serum; NC: Negative control; MOI: Multiplicity of infection; LVPW: Left ventricular posterior wall thickness; LVIDs: Left ventricular end-systolic diameter; LVEF: Left ventricular ejection fraction; HE: Hematoxylin–eosin; TUNEL: Terminal deoxynucleotidyl transferase-mediated deoxyuridine triphosphate-biotin nick end-labelin; ELISA: Enzyme-linked immunosorbent assay; TMB: Tetramethylbenzidine; TBS: Tris-buffered saline; ABC: Avidin–Biotin-Peroxidase Complex; OD: Optical density; RT-qPCR: Reverse transcription quantitative polymerase chain reaction; GAPDH: Glyceraldehyde-3-phosphate dehydrogenase; CTGF: Connective tissue growth factor; CCK: Cell counting kit; PI: Propidium iodide; ANOVA: Analysis of variance.

Supplementary Information

The online version contains supplementary material available at https://doi.org/10.1186/s11671-021-03559-2.

Additional file 1: Fig. 1. BMSC-derived exosomal miR-133 can reduce myocardial fibrosis in rats with VMC through suppressing MAML1.

Acknowledgements
We would like to acknowledge the reviewers for their helpful comments on this paper.

Authors' contributions
QL finished study design, QL, YJ, XY finished experimental studies, QL, WW, GD, XZ finished data analysis, QL finished manuscript editing. All authors read and approved the final manuscript.

Funding
The current research was funded by Zhejiang Province Ministry of Education (Grant/Award number: Y201839763) and Zhejiang Provincial Natural Science Foundation(Grant/Award number: LQ20H020005).

Declarations

Ethical approval
This study was approved and supervised by the animal ethics committee of The Fourth Affiliated Hospital of Zhejiang University School of Medicine. The treatment of animals in all experiments conforms to the ethical standards of experimental animals.

Consent for publication
Not applicable.

Competing interests
The authors declare that they have no competing interests.

Author details
[1]The Department of Cardiology, The Fourth Affiliated Hospital of Zhejiang University School of Medicine, N1 Shangcheng Road, Yiwu 322000, Zhejiang, China. [2]Nursing Department, The Fourth Affiliated Hospital of Zhejiang University School of Medicine, Yiwu 322000, Zhejiang, China. [3]The Ningbo Central Blood Station, Ningbo 315040, Zhejiang, China.

Received: 22 May 2020 Accepted: 31 May 2021
Published online: 02 July 2021

References

1. Fung G et al (2016) Myocarditis. Circ Res 118(3):496–514
2. Bruno KA et al (2019) BPA alters estrogen receptor expression in the heart after viral infection activating cardiac mast cells and T cells leading to perimyocarditis and fibrosis. Front Endocrinol (Lausanne) 10:598
3. Xiao Y et al (2019) Total Astragalus saponins attenuates CVB3-induced viral myocarditis through inhibiting expression of tumor necrosis factor alpha and Fas ligand. Cardiovasc Diagn Ther 9(4):337–345
4. Kindermann I et al (2012) Update on myocarditis. J Am Coll Cardiol 59(9):779–792
5. Zhang H et al (2019) Effects of ubiquitin-proteasome inhibitor on the expression levels of TNF-alpha and TGF-beta1 in mice with viral myocarditis. Exp Ther Med 18(4):2799–2804
6. Ji W et al (2019) miR-21 deficiency contributes to the impaired protective effects of obese rat mesenchymal stem cell-derived exosomes against spinal cord injury. Biochimie 167:171–178
7. Bostjancic E et al (2010) MicroRNAs miR-1, miR-133a, miR-133b and miR-208 are dysregulated in human myocardial infarction. Cardiology 115(3):163–169
8. Ferreira LR et al (2014) MicroRNAs miR-1, miR-133a, miR-133b, miR-208a and miR-208b are dysregulated in chronic chagas disease cardiomyopathy. Int J Cardiol 175(3):409–417
9. Besler C et al (2016) Endomyocardial miR-133a levels correlate with myocardial inflammation, improved left ventricular function, and clinical outcome in patients with inflammatory cardiomyopathy. Eur J Heart Fail 18(12):1442–1451
10. McDonald MK, Capasso KE, Ajit SK (2013) Purification and microRNA profiling of exosomes derived from blood and culture media. J Vis Exp 76:e50294
11. Boriachek K et al (2018) Biological functions and current advances in isolation and detection strategies for exosome nanovesicles. Small 14(6):1702153
12. Kowal J, Tkach M, Thery C (2014) Biogenesis and secretion of exosomes. Curr Opin Cell Biol 29:116–125
13. Tkach M, Thery C (2016) Communication by extracellular vesicles: where we are and where we need to go. Cell 164(6):1226–1232
14. Fan KL et al (2019) Altered exosomal miR-181d and miR-30a related to the pathogenesis of CVB3 induced myocarditis by targeting SOCS3. Eur Rev Med Pharmacol Sci 23(5):2208–2215
15. Zhu LP et al (2018) Hypoxia-elicited mesenchymal stem cell-derived exosomes facilitates cardiac repair through miR-125b-mediated prevention of cell death in myocardial infarction. Theranostics 8(22):6163–6177
16. Peng Y et al (2020) Exosomal miR-25-3p from mesenchymal stem cells alleviates myocardial infarction by targeting pro-apoptotic proteins and EZH2. Cell Death Dis 11(5):317
17. Emanueli C et al (2016) Coronary artery-bypass-graft surgery increases the plasma concentration of exosomes carrying a cargo of cardiac MicroRNAs: an example of exosome trafficking out of the human heart with potential for cardiac biomarker discovery. PLoS ONE 11(4):e0154274
18. Zhang J et al (2019) microRNA-193b protects against myocardial ischemia-reperfusion injury in mouse by targeting mastermind-like 1. J Cell Biochem 120(8):14088–14094
19. Zheng S et al (2018) Inhibition of Mastermind-like 1 alleviates liver fibrosis induced by carbon tetrachloride in rats. Exp Biol Med (Maywood) 243(14):1099–1108
20. Li Y et al (2020) Bone marrow mesenchymal stem cells-derived exosomal microRNA-185 represses ventricular remolding of mice with myocardial infarction by inhibiting SOCS2. Int Immunopharmacol 80:106156
21. Zhang ZF et al (2018) MicroRNA-1294 targets HOXA9 and has a tumor suppressive role in osteosarcoma. Eur Rev Med Pharmacol Sci 22(24):8582–8588
22. Pan X, Wang G, Wang B (2021) MicroRNA-1182 and let-7a exert synergistic inhibition on invasion, migration and autophagy of cholangiocarcinoma cells through down-regulation of NUAK1. Cancer Cell Int 21(1):161
23. Li W et al (2019) MiR-1/133 attenuates cardiomyocyte apoptosis and electrical remodeling in mice with viral myocarditis. Cardiol J 27(3):285–294
24. Li X et al (2019) Exosomes derived from cardiac progenitor cells attenuate CVB3-induced apoptosis via abrogating the proliferation of CVB3 and modulating the mTOR signaling pathways. Cell Death Dis 10(10):691
25. Alipoor SD et al (2016) Exosomes and exosomal miRNA in respiratory diseases. Mediators Inflamm 2016:5628404

26. Lin F et al (2019) YBX-1 mediated sorting of miR-133 into hypoxia/reoxygenation-induced EPC-derived exosomes to increase fibroblast angiogenesis and MEndoT. Stem Cell Res Ther 10(1):263
27. Xin H et al (2012) Exosome-mediated transfer of miR-133b from multipotent mesenchymal stromal cells to neural cells contributes to neurite outgrowth. Stem Cells 30(7):1556–1564
28. Chu Y et al (2018) Astragalus polysaccharides decrease proliferation, migration, and invasion but increase apoptosis of human osteosarcoma cells by up-regulation of microRNA-133a. Braz J Med Biol Res 51(12):e7665
29. Xiao Y et al (2019) MicroRNA-133a and myocardial infarction. Cell Transplant 28(7):831–838
30. Xu C et al (2014) beta-Blocker carvedilol protects cardiomyocytes against oxidative stress-induced apoptosis by up-regulating miR-133 expression. J Mol Cell Cardiol 75:111–121
31. Imamura K et al (2018) Released fibroblast growth factor18 from a collagen membrane induces osteoblastic activity involved with downregulation of miR-133a and miR-135a. J Biomater Appl 32(10):1382–1391
32. Ye H et al (2013) Nebivolol induces distinct changes in profibrosis microRNA expression compared with atenolol, in salt-sensitive hypertensive rats. Hypertension 61(5):1008–1013
33. Chen H et al (2019) Qiliqiangxin capsule improves cardiac function and attenuates cardiac remodeling by upregulating miR-133a after myocardial infarction in rats. Evid Based Complement Alternat Med 2019:7528214
34. Wang W et al (2019) Ginkgo biloba extract may alleviate viral myocarditis by suppression of S100A4 and MMP-3. J Med Virol 91(12):2083–2092
35. Wen ZQ et al (2019) LncRNA PEG10 aggravates cardiac hypertrophy through regulating HOXA9. Eur Rev Med Pharmacol Sci 23(3 Suppl):281–286

Publisher's Note